

Dynamic angiography of the Circle of Willis by arterial spin tagging

M. van Osch¹, J. Hendrikse¹, X. Golay², C. Bakker¹, J. van der Grond¹

¹University Medical Center Utrecht, Utrecht, Netherlands, ²National Neuroscience Institute, Singapore, Singapore

Introduction

The Circle of Willis (CoW) plays an important role in providing sufficient blood flow to the brain to meet metabolic demand. By means of MRA the geometrical structure of the CoW can be studied and phase contrast (PC) MRI can be used to estimate the blood flow and to identify flow direction. However, on directional flow images it is not possible to judge the importance of the collateral pathways and the accuracy of quantitative PC flow measurements is limited due to the small vessel size. Therefore, we propose the use of dynamic imaging of blood passing through the CoW to achieve a clear depiction of the blood flow through the CoW and to provide quantitative blood flow measurements in the main vessels of the CoW.

Methods

Dynamic angiographic imaging of the CoW is achieved by the inversion of spins in a slab proximal to the imaging plane.¹ Acquisition is performed by using a train of multiple small angle pulses and segmented EPI-readout. Selective visualization of the vessels is achieved by the complex subtraction of the labeled images from control images that are acquired in the same manner but without the selective inversion of spins. Additionally, the input profile of the labeled spins into the CoW is measured in the internal carotid arteries (ICAs) and the basilar artery (BA) using the same labeling slab with a thinner imaging slice.

The TURBO-TILT sequence is used for acquisition (Fig. 1), with a 70 mm labeling slab and a 25 mm imaging slice through the CoW (FOV=240 mm, TE=5 ms, TR=1 s, 256x256 matrix, halfscan (60%), $\alpha = 25^\circ$, $\Delta t=11.5$ ms).² For quantitative flow measurements an input function measurement is performed with a 5 mm image slice through the carotid arteries just below the skull base ($\alpha=60^\circ$, 2 averages), followed by two interleaved scans for the measurement of the passage through the Circle of Willis with the labeling slice at the same position as for the input measurement ($\Delta t_{\text{first}}=16$ and 27.5 ms, $\alpha=17.5^\circ$, $\Delta t=23$ ms, 12 averages, with cardiac triggering).

Post-processing

The qualitative images are shown as a movie and by identification of the moment of maximum inflow of labeled spins a time-of-arrival map is made. Quantification of the blood flow is possible by averaging the blood passages over a region-of-interest (ROI) of an artery. The T_1 -decay of the difference magnetization is subsequently modeled as ($T_{1,\text{eff}}$ is Look-Locker T_1):

$$\Delta M(t) = 2 \cdot M_0 \cdot \exp\left(-t\left(\beta \cdot T_1^{\text{blood}^{-1}} + (1-\beta)T_{1,\text{eff}}^{\text{blood}^{-1}}\right)\right), \text{ with } 1-\beta \text{ the time that spins experience pulses.}$$

When assuming plug flow, the total number of spins present in the ROI can be calculated as the number of spins that entered during the transit time of the ROI (\bar{t}):

$$n_{\text{CoW}}^{\text{ROI}}(t) = \text{BF}_{\text{CoW}} \cdot \int_{t-\bar{t}}^t c_{\text{input}}(t') dt' \approx \text{BF}_{\text{CoW}} \cdot \int_{t-\bar{t}}^{t-\text{TA}} c_{\text{CA}}(t') dt' = \frac{\text{BF}_{\text{CoW}}}{V_{\text{CA}}} \cdot \int_{t-\bar{t}}^{t-\text{TA}} n_{\text{CA}}(t') dt'$$

flow, TA the time-of-appearance, $c_{\text{input}}(t)$ the number of labeled spins per unit blood volume that entered the ROI, $c_{\text{CA}}(t)$ is the input function and V_{CA} is the volume of voxels of the input measurement (assuming pure blood voxels). The blood flow is finally calculated by iteratively minimizing the error term ϵ as a function of BF_{CoW} , TA, \bar{t} , and background noise η :

$$\epsilon = \sum_{t=0}^{N-1} \left(\frac{S_{\text{CoW}}^{\text{ROI}}(t) - \eta}{\exp\left(-t\left(\beta \cdot T_1^{\text{blood}^{-1}} + (1-\beta)T_{1,\text{eff}}^{\text{blood}^{-1}}\right)\right)} - \frac{\text{BF}_{\text{CoW}}}{V_{\text{CA}}} \cdot \int_{t-\bar{t}}^{t-\text{TA}} \frac{S_{\text{CA}}(t')}{\exp\left(-t' \cdot T_1^{\text{blood}^{-1}}\right)} dt' \right)^2$$

Results and Discussion

Fig. 2 shows the application of qualitative dynamic angiography in a patient with a right-sided occluded ICA. Both dynamic images and arrival-time-map show that the right MCA is fed by the posterior circulation. When comparing the true flow in a phantom with the quantitative flow measurements by dynamic angiography, a highly significant correlation is found, although the flow is underestimated by 15% (Fig. 3). Several reasons may explain this effect. First, the input function only approximates the true input of the ROI in the CoW. Its dispersion would result in underestimating BF, owing to the broadening of the response function. Second, a too high β could equally well explain a low BF. Finally, it could be explained by joined fitting of the transit time through the ROI and the amplitude of the boxcar function.

An in vivo comparison with PC flow measurements shows a good general agreement, although the spread in flow values is larger (Table 1). The biggest advantages of the proposed method over PC flow quantification are its insensitivity to partial volume artifacts and the simultaneous measurement of the flow in the MCAs, the posterior cerebral arteries (PCAs) and the anterior circulation. Because of the subtraction of label and control images, solely the blood signal is imaged, thus enabling the quantitative measurement of the amount of labeled blood unaffected by partial volume effects. Principle limitation of the technique is that there should be considerable delay differences within an ROI or pixel to measure the flow. This will restrict the analysis to anatomical structures, like the CoW that can easily be imaged in a single, thick slab image. Another drawback of the technique is that it relies on the measurements of an input function that will result in a larger spread of flow values (e.g. due to a non-orthogonal planning). This might necessitate the use of three separate input function measurements.

¹Warmuth C et al. ISMRM 2001, p. 1559 ²Hendrikse J et al, Magn Reson Med 2003, p. 429-433

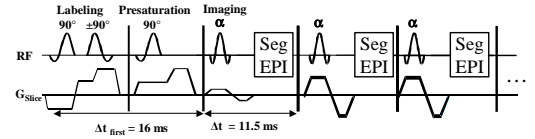


Figure 1: Pulse diagram for dynamic angiography.

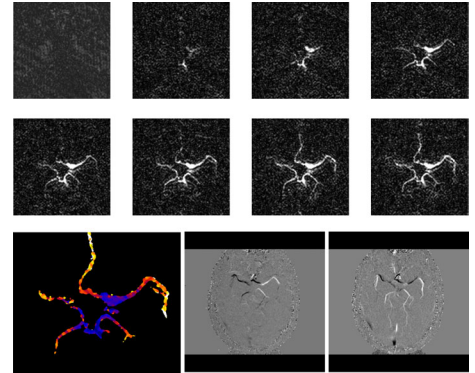


Figure 2: Dynamic angiography of a patient with an occlusion of the right internal carotid artery and collateral flow via the right posterior cerebral artery and posterior communicating artery. Only every 4th image is shown (39, 85, ..., 361 ms). Lower row: time-of-arrival (left) and directional flow in the L-R and A-P direction (right).

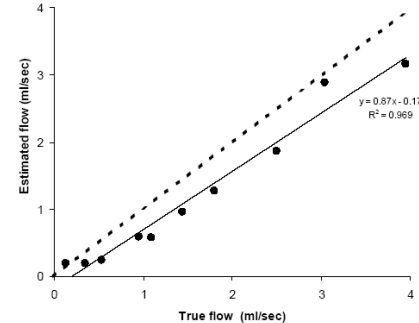


Figure 3: Comparison of the estimated flow by dynamic angiography through the left MCA of a Circle of Willis phantom and the true flow as measured by the collected volume principle. Dashed line indicates line of identity.

Table 1: Flow measurements by dynamic angiography in three normal volunteers in the MCA (averaged over all left and right MCAs), PCA (averaged over all left and right PCAs), the anterior cerebral arteries (ACAs, summed flow through the left and right ACA). Flow values are indicated as mean \pm standard error of the mean. Flow in ml/s.

	MCA	PCA	ACA _L + ACA _R	Total anterior	Total posterior
Flow by dynamic angiography	2.56 \pm 0.48	1.20 \pm 0.14	3.16 \pm 0.36	8.3 \pm 1.4 ^a	2.40 \pm 0.34 ^c
Flow by PC-MRI	2.36 \pm 0.10	-	-	11.3 \pm 1.4 ^b	2.95 \pm 0.51 ^d

^aMCA_L+MCA_R+ACAs; ^bICA_L+ICA_R; ^cPCA_L+PCA_R; ^dBA